

# Preparation, Characterization, and FET Properties of Novel Dicyanopyrazinoquinoxaline Derivatives

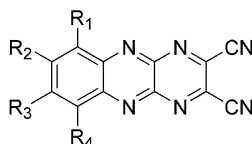
Jun-ichi Nishida, Naraso, Shio Murai, Eiichi Fujiwara,<sup>†</sup> Hirokazu Tada,<sup>†</sup> Masaaki Tomura,<sup>†</sup> and Yoshiro Yamashita\*

Department of Electronic Chemistry, Interdisciplinary Graduate School of Science and Engineering, Tokyo Institute of Technology, Nagatsuta, Midori-ku, Yokohama 226-8502, Japan, and Institute for Molecular Science, Myodaiji, Okazaki 444-8585, Japan

yoshiro@echem.titech.ac.jp

Received April 1, 2004

## ABSTRACT



A series of the title dicyanopyrazinoquinoxaline derivatives have been prepared and characterized by using single-crystal X-ray structure analysis and redox potential measurements. They have strong electron-accepting properties due to the pyrazinopyrazine skeletons as well as the cyano groups. Substituents can be easily introduced at the benzene ring and control the HOMO–LUMO energy gap and the molecular packing. They show clear n-type transistor properties in the FET devices.

Recently, there has been increased interest in organic and polymeric thin-film field-effect transistors (FETs) due to their potential application to low-cost electronic devices and their circuits.<sup>1</sup> To date, there are many reports on FETs with p-type characteristics such as pentacene and thiophene oligomers with high hole mobilities on Si/SiO<sub>2</sub>,<sup>2,3</sup> whereas a limited number of compounds have been found to function as n-type semiconductors. Air-stable n-type semiconducting materials are important components of the p–n junction diodes and bipolar transistors.<sup>4</sup> Diimide derivatives,<sup>5</sup> oligothiophenes possessing fluorinated substituents,<sup>6</sup> metallophthalocyanines,<sup>7</sup> and hetero-tetracyanoquinodimethanes<sup>8</sup> are prominent examples of n-type materials. These molecules contain  $\pi$ -

extended units that work as p-type semiconductors. This fact suggests that modification of  $\pi$ -conjugated systems used for p-type transistors would afford novel n-type ones.

Pentacene shows the highest hole mobility because its linear fused ring structure with extended  $\pi$ -conjugation and rigid planarity is suitable for intermolecular  $\pi$ – $\pi$  overlap and face-to-edge interactions in the solid state.<sup>9</sup> Several analogues of pentacene have been developed to improve the properties.<sup>10</sup> However, acene compounds showing n-type

<sup>†</sup> Institute for Molecular Science.

(1) (a) Katz, H. E. *J. Mater. Chem.* **1997**, 7, 369–376. (b) Horowitz, G. *Adv. Mater.* **1998**, 10, 365–377. (c) Voss, D. *Nature* **2000**, 407, 442–444.

(2) (a) Gundlach, D. J.; Lin, Y. Y.; Jackson, T. N.; Nelson, S. F.; Schlom, D. G. *IEEE Electron Device Lett.* **1997**, 18, 87–89. (b) Klauk, H.; Halik, M.; Zschieschang, U.; Schmid, G.; Radlik, W.; Weber, W. *J. Appl. Phys.* **2002**, 92, 5259–5263.

(3) (a) Dodabalapur, A.; Torsi, L.; Katz, H. E. *Science* **1995**, 268, 270–271. (b) Dimitrakopoulos, C. D.; Furman, B. K.; Graham, T.; Hegde, S.; Purushothaman, S. *Synth. Met.* **1998**, 92, 47–52. (c) Katz, H. E.; Lovinger, A. J.; Laquindanum, J. G. *Chem. Mater.* **1998**, 10, 457–459.

(4) (a) Crone, B.; Dodabalapur, A.; Lin, Y.-Y.; Filas, R. W.; Bao, Z.; Laduca, A.; Sarpeshkar, R.; Katz, H. E.; Li, W. *Nature* **2000**, 403, 521–523. (b) Dimitrakopoulos, C. D.; Malenfant, P. R. L. *Adv. Mater.* **2002**, 14, 99–117. (c) Würthner, F. *Angew. Chem., Int. Ed.* **2001**, 40, 1037–1039.

(5) Katz, H. E.; Lovinger, A. J.; Johnson, J.; Kloc, C.; Siegrist, T.; Li, W.; Lin, Y.-Y.; Dodabalapur, A. *Nature* **2000**, 404, 478–481.

(6) (a) Facchetti, A.; Deng, Y.; Wang, A.; Koide, Y.; Sirringhaus, H.; Marks, T. J.; Friend, R. H. *Angew. Chem., Int. Ed.* **2000**, 39, 4547–4551. (b) Facchetti, A.; Yoon, M.-H.; Stern, C. L.; Katz, H. E.; Marks, T. J. *Angew. Chem., Int. Ed.* **2003**, 42, 3900–3903.

(7) Bao, Z.; Lovinger, A. J.; Brown, J. J. *Am. Chem. Soc.* **1998**, 120, 207–208.

(8) Chesterfield, R. J.; Newman, C. R.; Pappenfus, T. M.; Ewbank, P. C.; Haukaas, M. H.; Mann, K. R.; Miller, L. L.; Frisbie, C. D. *Adv. Mater.* **2003**, 15, 1278–1282.

transistor properties are still rare. This is probably due to the weak electron-accepting properties of pentacene analogues. On the other hand, nitrogen-containing heterocycles such as pyrazines are known as electron-accepting compounds.

In this context, novel unique acene molecules containing nitrogen atoms, dicyanopyrazinoquinoxaline derivatives, have now been designed as n-type transistor materials. They have the following advantages: (1) They contain a  $\pi$ -conjugated system that would lead to efficient intermolecular interactions. (2) They have strong electron-accepting properties due to the pyrazinopyrazine skeletons as well as the cyano groups. (3) The cyano groups may be useful for negative-charge injection as suggested in a compound possessing pentafluorobenzene groups.<sup>6b</sup> (4) Substituents can be easily introduced at the benzene ring to control the HOMO–LUMO energy gap and the molecular packing. Introduction of electron-donating groups would lead to a donor–acceptor compound, where a highly polarized structure is considered to be favorable for the  $\pi$ – $\pi$  stacking. Ambipolar properties are also expected in such donor–acceptor compounds.<sup>8</sup> We report herein the synthesis and characterization of dicyanopyrazinoquinoxaline **1a–d** and  $\pi$ -extended analogues **1e,f**. FETs using them have been fabricated, and their performances as n-type semiconductors are presented. The com-

reaction of phenanthrene-9,10-dione with 2,3-diamino-5,6-dicyanopyrazine. Phenanthrene derivative **2** was prepared for comparison.<sup>12</sup> These compounds exhibited high decomposition points at 248–365 °C and could be purified by sublimation.

According to the PM3 calculations,<sup>13</sup> the LUMO of dicyanopyrazinoquinoxaline is localized on the pyrazinoquinoxaline ring, and the HOMO is localized on the benzene ring as shown in Figure 1. Therefore, the introduction of

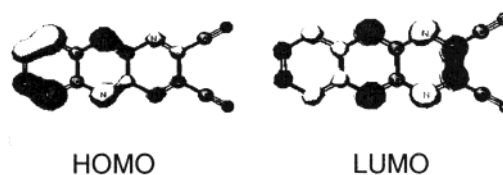
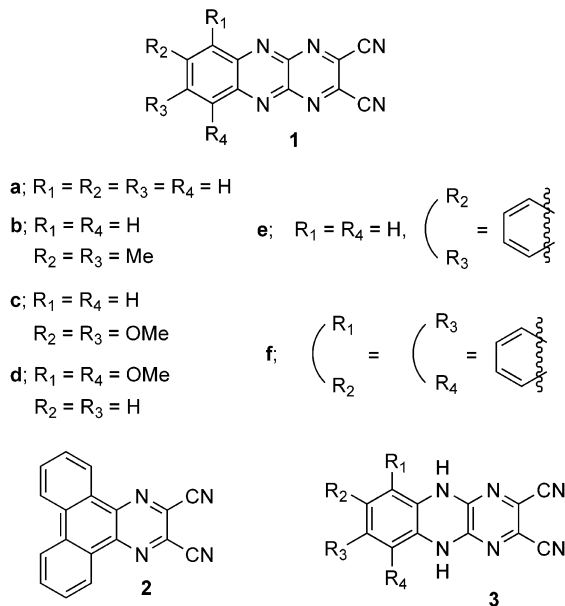


**Figure 1.** HOMO and LUMO of **1a** calculated by the PM3 method.

**Scheme 1.** Dicyanopyrazinoquinoxaline Derivatives



pounds **1a,b** were prepared in 95% and 93% yields by treating diamino precursors **3a,b**<sup>11</sup> with 2,3-dichloro-5,6-dicyano-*p*-benzoquinone (DDQ). Diamino compounds **3c,d** bearing methoxy groups and **3e** were prepared by the nucleophilic reaction of the corresponding diamines with 2,3-dichloro-5,6-dicyanopyrazine in 70%, 51%, and 61% yields, respectively. Their oxidation reactions using DDQ gave **1c–e** in 79%, 80%, and 84% yields, respectively. Phenanthrene derivative **1f** was prepared in 94% yield by the condensation

substituents on the benzene ring is considered to affect the HOMO. As the result, introduction of electron-donating groups would increase only the HOMO, resulting in reduced HOMO–LUMO gaps. This is supported by the absorption spectra. Compound **1a** exhibits the absorption maxima at 398 nm, whereas the absorption maxima of methyl and methoxy derivatives **1b,c** are observed at longer wavelengths as a result of the electron-donating substituents. Interestingly, compound **1d** having methoxy groups shows a weak intramolecular CT band at 628 nm. The similar weak CT band (631 nm) is observed in compound **1e** with an extra benzene ring. In the case of phenanthrene derivative **1f**, the absorption maximum is observed at a wavelength ca. 50 nm longer than that of the comparison compound **2**, indicating the low LUMO energy of the pyrazinopyrazine unit. These absorption maxima are summarized in Table 1.

The electron-accepting properties were investigated by cyclic voltammetry. All of the voltammograms exhibited reversible two-stage one-electron reduction waves (Table 1). The first reduction potential of **1a** is comparable to that of chloranil (0 V vs SCE), indicating the strong electron-accepting property. The reduction potentials of **1b–d** are observed at potentials lower than those of **1a**, indicating that the introduction of electron-donating methyl and methoxy groups at the benzene ring lowers the reduction potentials. It should be noted here, however, that the shifted values are

(9) (a) Siegrist, T.; Kloc, C.; Schön, J. H.; Batlogg, B.; Haddon, R. C.; Berg, S.; Thomas, G. A. *Angew. Chem., Int. Ed.* **2001**, *40*, 1732–1736. (b) Mattheus, C. C.; Wijs, G. A.; Groot, R. A.; Palstra, T. T. M. *J. Am. Chem. Soc.* **2003**, *125*, 6323–6330. (c) Brinkmann, M.; Graff, S.; Straupé, C.; Wittmann, J.-C.; Chaumont, C.; Nuesch, F.; Aziz, A.; Schaer, M.; Zuppiroli, L. *J. Phys. Chem. B* **2003**, *107*, 10531–10539.

(10) (a) Laquindanum, J. G.; Katz, H. E.; Lovinger, A. J. *J. Am. Chem. Soc.* **1998**, *120*, 664–672. (b) Miao, Q.; Nguyen, T.-Q.; Someya, T.; Blanchet, G. B.; Nuckolls, C. J. *J. Am. Chem. Soc.* **2003**, *125*, 10284–10287.

(11) Ried, W.; Tsiotis, G. *Liebigs Ann. Chem.* **1988**, 1197–1199.

(12) Van der Tol, E. B.; Van Ramesdonk, H. J.; Verhoeven, J. W.; Streemers, F. J.; Kerver, E. G.; Verboom, W.; Reinhoudt, D. N. *Chem. Eur. J.* **1998**, *4*, 2315–2323.

(13) (a) Stewart, J. J. P. *J. Comput. Chem.* **1989**, *10*, 209–220. (b) Stewart, J. J. P. *J. Comput. Chem.* **1989**, *10*, 221–264.

**Table 1.** Redox Potentials<sup>a</sup> and Optical Properties<sup>b</sup>

	$E_1^{\text{red}}$ (V)	$E_2^{\text{red}}$ (V)	$E_1^{\text{ox}}$ (V)	$\lambda_{\text{max}}$ (nm); log $\epsilon$
<b>1a</b>	−0.03	−0.87		398; 4.45
<b>1b</b>	−0.12	−0.88		411; 4.45
<b>1c</b>	−0.27	−0.98		427; 4.45
<b>1d</b>	−0.07	−0.93	+1.48	388; 3.71, 628; 3.00
<b>1e</b>	+0.10	−0.66		451; 4.14, 631; 2.96
<b>1f</b>	−0.20	−0.98		435; 4.43
<b>2</b>	−1.01			388; 3.94

<sup>a</sup>  $E/V$  vs SCE in  $\text{CH}_2\text{Cl}_2$ , 0.1 mol  $\text{dm}^{-3}$   $n\text{-Bu}_4\text{NPF}_6$ , Pt electrode, scan rate 100 mVs<sup>−1</sup>. <sup>b</sup> In  $\text{CH}_2\text{Cl}_2$ .

not so large and their electron affinity is still high. This is attributed to the electronic structure, where the LUMO is localized on the pyrazinopyrazine unit. In the case of **1d**, the reduction potentials are highest among the derivatives **1b–d** and even the oxidation peak is observed. This amphoteric redox property is related to the CT band observed in the absorption spectrum and is interesting for the fabrication of ambipolar semiconductors. Reduction waves of naphthalene derivative **1e** appear at higher potentials. The first reduction potential (+0.10 V) is comparable to that of thiopheneTCNQ. Phenanthrene derivative **1f** exhibits reduction potentials lower than those of **1a**, indicating that the linear acene structure attributes to lowering the LUMO levels. On the other hand, comparison compound **2** showed only one reduction peak at a lower potential. This fact shows that the pyrazinopyrazine unit is essential for the strong electron-accepting properties.

X-ray analysis<sup>14</sup> of **1a–d** revealed planar molecular structures and herringbone structures with a close face-to-edge (T-shape) packing as shown in Figure 2. In the crystal structure of **1a**, the molecules are arranged in a typical herringbone motif like that of pentacene as shown in Figure 2a.<sup>9</sup> Interestingly, a molecular tape structure is formed with C–H $\cdots$ N intermolecular contacts along the *b* axis (Figure 2b), where the C $\cdots$ N distances are 3.407(3) and 3.730(3) Å. The dimethoxy derivative **1c** has a similar herringbone structure, although the tape-like network is not formed, where the distances between the cyano-nitrogen and the benzene-carbon are 5.98 and 6.83 Å, respectively. On the other hand, face-to-face packing patterns appear in the derivatives **1b** and **1d**. Dimethyl derivative **1b** forms a dimer unit, which

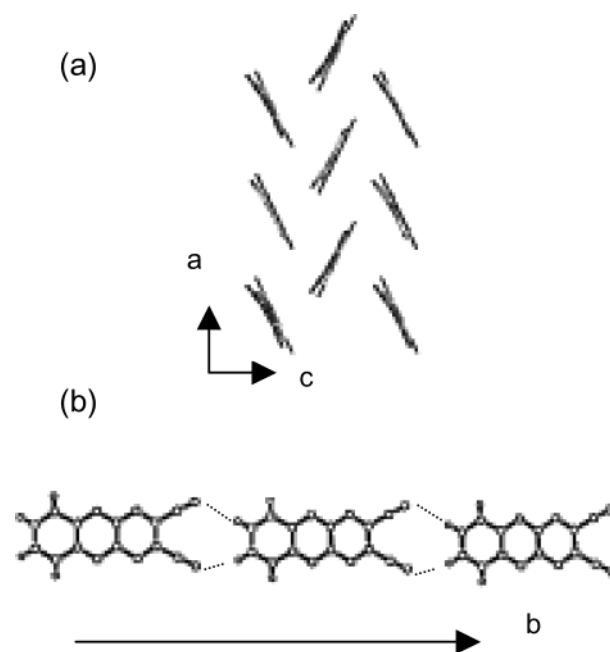


**Figure 2.** Crystal packing of **1a**. (a) Viewed along the *b* axis with the dihedral angle between the two molecular planes of 55.7(1)°. (b) Molecular tape structure with C–H $\cdots$ N contacts along the *b* axis.

is arranged in a herringbone manner. In the crystal structure of **1d**, both types of overlaps of the molecules (face-to-face and face-to-edge) are observed, in which the cofacial  $\pi$ – $\pi$  distances are 3.395 and 3.496 Å. This may be related to the higher HOMO and lower LUMO levels resulting in the strong  $\pi$ – $\pi$  interactions. In the neighboring face-to-edge columns, a methoxy group in this compound is located between the cyano groups of the neighboring molecules, leading to a close intermolecular distance (3.25 Å). X-ray analysis on phenanthrene derivative **2** was also carried out. A one-dimensional columnar structure of **2** suggests that phenanthrene derivatives predominantly form stacking structures.

FETs using the dicyanopyrazinoquinoxaline derivatives were fabricated on  $\text{SiO}_2/\text{Si}$  substrates by a high-vacuum evaporation method ( $10^{-6}$ – $10^{-7}$  Torr) with bottom contact

(14) Crystal data for **1a**:  $\text{C}_{12}\text{H}_4\text{N}_6$ , MW = 232.21, orthorhombic  $Pca2_1$ ,  $a = 11.540(4)$ ,  $b = 12.515(5)$ ,  $c = 6.974(2)$  Å,  $V = 1007.2(6)$  Å<sup>3</sup>,  $Z = 4$ ,  $D_{\text{calc}} = 1.531$  g/cm<sup>3</sup>,  $R_1 = 0.0531$ ,  $wR_2 = 0.1252$ ,  $S = 1.164$ . For **1b**:  $\text{C}_{14}\text{H}_8\text{N}_6$ , MW = 260.26, orthorhombic  $Pbca$ ,  $a = 11.9547(9)$ ,  $b = 7.5468(5)$ ,  $c = 26.455(2)$  Å,  $V = 2386.8(6)$  Å<sup>3</sup>,  $Z = 8$ ,  $D_{\text{calc}} = 1.448$  g/cm<sup>3</sup>,  $R_1 = 0.082$ ,  $wR_2 = 0.215$ ,  $S = 2.38$ . For **1c**:  $\text{C}_{14}\text{H}_8\text{O}_2\text{N}_6$ , MW = 292.26, orthorhombic  $P2_12_12_1$ ,  $a = 5.964(3)$ ,  $b = 7.229(4)$ ,  $c = 30.65(2)$  Å,  $V = 1321(1)$  Å<sup>3</sup>,  $Z = 4$ ,  $D_{\text{calc}} = 1.469$  g/cm<sup>3</sup>,  $R_1 = 0.055$ ,  $wR_2 = 0.125$ ,  $S = 1.58$ . For **1d**:  $\text{C}_{14}\text{H}_8\text{N}_6\text{O}_2 \cdot (\text{H}_2\text{O})_{0.25}$ , MW = 296.77, monoclinic  $C2$ ,  $a = 27.168(3)$ ,  $b = 9.4308(9)$ ,  $c = 21.837(2)$  Å,  $\beta = 99.836(8)^\circ$ ,  $V = 5512.7(10)$  Å<sup>3</sup>,  $Z = 16$ ,  $D_{\text{calc}} = 1.430$  g/cm<sup>3</sup>,  $R_1 = 0.0699$ ,  $wR_2 = 0.1814$ ,  $S = 0.996$ . For **2**:  $\text{C}_{18}\text{H}_8\text{N}_4$ , MW = 280.29, monoclinic  $P2_1/c$ ,  $a = 10.239(6)$ ,  $b = 7.217(5)$ ,  $c = 19.797(8)$  Å,  $\beta = 115.17(5)^\circ$ ,  $V = 1323(1)$  Å<sup>3</sup>,  $Z = 4$ ,  $D_{\text{calc}} = 1.406$  g/cm<sup>3</sup>,  $R_1 = 0.067$ ,  $wR_2 = 0.153$ ,  $S = 0.96$ .

(15) The film of **1f** did not show the FET property on a Au electrode. The film of **1a** showed almost the same FET properties on Au and Al electrodes.

**Table 2.** Mobilities and  $I_{\text{on}}/I_{\text{off}}$  Ratios<sup>a</sup>

	mobilities (cm <sup>2</sup> /V·s)	$I_{\text{on}}/I_{\text{off}}$
<b>1a</b>	$3.6 \times 10^{-6}$	$10^3$
<b>1b</b>	$1.0 \times 10^{-8}$	10
<b>1c</b>	$2.1 \times 10^{-7}$	$10^2$
<b>1d</b>	$2.5 \times 10^{-7}$	$10^2$
<b>1e</b>	$2.2 \times 10^{-6}$	$10^2$
<b>1f</b>	$9.6 \times 10^{-7}$	$10^2$
<b>2</b>	–	–

<sup>a</sup> Fabricated on Au bottom electrodes except for **1f**, which was on an Al electrode.<sup>15</sup>

geometries at room temperature. The FET measurements were carried out in situ, and the results are summarized in Table 2. No attempts were made to optimize the performances through changing substrate temperatures or film morphology. Figure 3 shows the output characteristics for

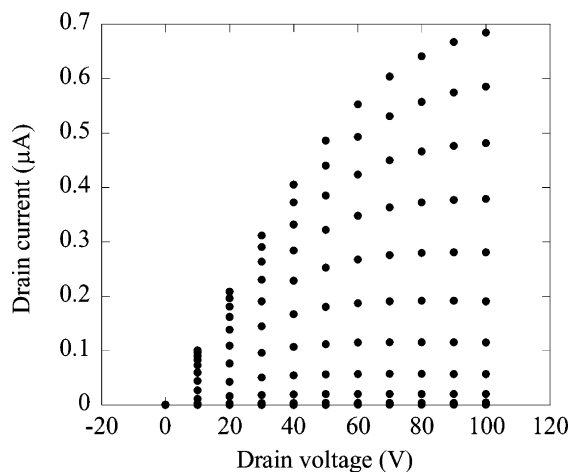


**Figure 3.** FET characteristics for the film of **1a** (100 nm) deposited at room temperature. Gate voltages were 0–100 V from bottom to top curves in increments of 10 V.

**1a-FET.** The channel conductance increases as  $V_g$  becomes more positive, meaning that the film is an n-type conductor. Other derivatives **1b–f** also showed n-type FET characteristics and the electron mobilities were  $10^{-6}$ – $10^{-8}$   $\text{cm}^2 \text{V}^{-1} \text{s}^{-1}$  (Table 2). This result shows that the dicyanopyrazinoquinoxaline unit plays a fundamental role in establishing the active conducting channel. The introduction of methyl or methoxy substituents decreased the mobilities slightly. This

may be related to the crystal structures since the steric interactions between molecules are less in the crystal of **1a**, forming a tape-like network. Although dimethoxy derivatives **1c** and **1d** have different electronic and crystal structures, the mobilities are almost the same. Introduction of longer alkyl groups might make a clear difference depending on the substituent position. The  $\pi$ -extended naphthalene derivative **1e** having the lowest LUMO energy did not improve the mobility significantly. This fact indicates that the electron-accepting ability is not directly related to the mobility in the FET devices. However, the fact that pyrazine derivative **2** did not show any FET characteristics indicates that some electron-accepting properties are necessary for producing the active conducting channel.

In conclusion, novel dicyanopyrazinoquinoxalines with high electron affinity were prepared by a simple method. The electronic properties were tuned by introducing substituents at the benzene rings. Unique crystal packings were observed in the single crystals. Their active layers showed clean n-type transistor performances. These are the first examples of n-type FET based on pyrazinoacene-type molecules. To improve the FET properties, studies using new dicyanopyrazinoquinoxaline derivatives with higher symmetry and higher polarized structures are now in progress.

**Acknowledgment.** This work was supported by The 21st Century COE program and a Grant-in-Aid for Scientific Research or Priority Areas (no. 15073212) and “Nanotechnology Support Project” of the Ministry of Education, Culture, Sports, Science and Technology, Japan.

**Supporting Information Available:** Detailed experimental procedure, UV–vis spectra of compounds **1a–f** and **2**, and crystal structures of **1b–d** and **2**. This material is available free of charge via the Internet at <http://pubs.acs.org>.

OL0494010